Magnetite biomineralization in the human brain

(Iron/extremely low frequency magnetic fields)

JOSEPH L. KIRSCHVINK, ATSUKO KOBAYASHI-KIRSCHVINK, AND BARBARA J. WOODFORD*

Division of Geological and Planetary Sciences, The California Institute of Technology, Pasadena, CA 91125

ABSTRACT Although the mineral magnetite (Fe_3O_4) is precipitated biochemically by bacteria, protists, and a variety of animals, it has not been documented previously in human tissue. Using an ultrasensitive superconducting magnetometer in a clean-lab environment, we have detected the presence of ferromagnetic material in a variety of tissues from the human brain. Magnetic particle extracts from solubilized brain tissues examined with high-resolution transmission electron microscopy, electron diffraction, and elemental analyses identify minerals in the magnetite–maghemite family, with many of the crystal morphologies and structures resembling strongly those precipitated by magnetotactic bacteria and fish. These magnetic and high-resolution transmission electron microscopy measurements imply the presence of a minimum of 5 million single-domain crystals per gram for most tissues in the brain and >100 million crystals per gram for pia and dura. Magnetic property data indicate the crystals are in clumps of between 50 and 100 particles. Biogenic magnetite in the human brain may account for high-field saturation effects observed in the T1 and T2 values of magnetic resonance imaging and, perhaps, for a variety of biological effects of low-frequency magnetic fields.

In past studies of iron storage and magnetic resonance imaging (MRI), it has been assumed universally that there are no permanently magnetized (ferromagnetic) materials present in human tissues (1, 2). Similar assumptions have been made in virtually all biophysical assessments of human risk associated with exposure to static and extremely low-frequency magnetic fields (3) and by critics (4) of epidemiological studies that suggest links between weak power-line-frequency magnetic fields and various human disorders (5, 6). These analyses have focused on the side effects of electrical induction or possible diamagnetic and paramagnetic interactions. However, the ferrimagnetic mineral magnetite (Fe_3O_4) is formed biochemically by many living organisms. Because ferromagnetic crystals interact more than a million times more strongly with external magnetic fields than do diamagnetic or paramagnetic materials of similar volume, earth-strength magnetic fields can yield many responses that stand above thermal noise (7). Hence, the assumption implicit in past studies that human tissues are free of ferromagnetic material needs to be reassessed critically and tested experimentally.

Previous searches for biogenic magnetite in human tissues have not been conclusive (8, 9). Despite this, extensive research over the past 30 years has demonstrated that many organisms have the biochemical ability to precipitate the ferrimagnetic minerals magnetite (Fe_3O_4) (10–16) and greigite (Fe_3S_4) (17). In terms of its phyletic distribution, magnetite biomineralization is particularly widespread, having been documented in monerans (10), protists (11), and animals (12–16), with a fossil record extending back into Precambrian time (18). Within Kingdom Animalia, it is known within the mollusks (12), arthropods (13), and chordates (14, 15) and is suspected in many more groups (16). In the microorganisms (10, 11) and fish (15), linear chains of membrane-bound crystals of magnetite (magnetosomes) form structures best described as "biological bar magnets."

We report here that human tissues possess similar crystals of biogenic magnetite, with minimum estimates between 5 and 100 million single-domain crystals per gram in the tissues of the human brain. Magnetic particle extracts from solubilized tissues examined with high-resolution transmission electron microscopy (TEM) and electron diffraction identify minerals in the magnetite–maghemite solid solution, with many crystal morphologies and structures resembling those precipitated by magnetotactic bacteria and fish.

MATERIALS AND METHODS

Tissue Samples. Human brain material was obtained 12–24 h postmortem from the Alzheimer's Disease Research Center Consortium of Southern California. Samples of brain and meninges were dissected using acid-cleaned ceramic or Teflon-coated instruments. These tissues were placed into 70% ethanol [made with deionized water and filtered through a 200-nm (pore-size) Millipore filter] in containers that had previously been cleaned with 2 M HCl. Samples from seven brains were obtained from patients whose ages averaged 65 years and ranged from 48 to 88 years. Four of these were from suspected Alzheimer disease patients. Cerebral cortical areas and cerebellum were included for all seven brains. In one case, brain and spinal dura, basal ganglia, and midbrain and, in another case, olfactory bulbs, superior sagittal sinus, and tentorium of the dura were obtained in addition to the above tissues.

Magnetometry. Subsamples for magnetic measurements were removed from the tissues by using similar tools in a magnetically shielded dust-free clean laboratory (19). Measurements of ferromagnetic materials were made using a magnetometer employing Rf-biased superconducting quantum interference devices (SQUIDs), designed to measure the total ferromagnetic *moment* of samples placed within a Helmholtz-coil pickup loop (20). Samples were fastened to a thin acid-washed monofilament string, and a stepping motor moved the sample vertically between the magnetization and demagnetization coils and the measurement region of the SQUID magnetometer. Several magnetic analyses borrowed from the field of rock and mineral magnetism (21–23) were performed routinely on frozen tissue samples to determine the concentration, mineralogy, and packing geometry of any ferromagnetic materials present.

Abbreviations: MRI, magnetic resonance imaging; SQUID, superconducting quantum interference device; TEM, transmission electron microscopy; IRM, isothermal remanent magnetization; ARM, anhysteretic remanent magnetization.
*Present address: Department of Anatomy and Cell Biology, University of Southern California, 1333 San Pablo Street, Los Angeles, CA 90033.

Sample Preparation for the Magnetometer. Pia and blood vessels were removed from all samples of the meninges before analysis in the SQUID magnetometer. Two preparation methods were used. Large intact samples of the cerebral cortex and cerebellum were frozen directly in liquid nitrogen. Brain tissues that fractured upon freezing or dissection were placed into a previously acid-cleaned ice-cube mold and frozen into blocks with small quantities of nonmagnetic deionized water. Either the frozen piece of brain or the ice/brain block was attached by a slip knot to the monofilament line and then centered within the column of the SQUID magnetometer. Background instrument noise and the levels of laboratory contaminants were monitored with blank 15-g ice cubes of distilled deionized water; typical ice-cube background noise levels were in the range of 2×10^{-8} A·m²·kg⁻¹. All aqueous solutions used in sample handling were passed through 200-nm filters. All solutions, including the toluene and tissue solubilizers, were cleaned magnetically by storing for at least 2 weeks prior to use in containers with large high-intensity NdFeB magnets strapped to their base to aid in the removal of any preexisting ferromagnetic contaminants.

Extraction and Electron Microscopy. Extraction devices made from Pyrex weighing vials were used to remove the magnetic particles from the brain tissues. The ground-glass caps were modified by glass blowing to make a thin-walled cylindrical finger, sealed on the bottom, extending from the cap about ⅔ of the distance into the vial. Tissues were digested in magnetically cleaned commercial solutions of toluene/quaternary ammonium hydroxide (e.g., Beckman tissue solubilizer), ≈1:5 (vol/vol) for a minimum period of 1 week while exposed to the strong field of a NdFeB magnet inserted within the finger. The vial cap and magnetic finger were then rinsed in clean toluene, the magnetic aggregates were redispersed mechanically in 0.25 ml of toluene, and small drops were placed on carbon-coated copper grids for high-resolution TEM analysis. Samples were examined at high resolution on a Phillips model 430 300-kV high-resolution TEM with an energy-dispersive x-ray analysis system for elemental determinations. Mineralogic assign-

ments were made by indexing the spot patterns produced by selected-area electron diffraction on individual mineral grains and on rings from powder patterns, with calibration against a gold film standard. An estimate of the grain-size distribution was made by measuring the length and width of 70 crystal shadows from a large clump. Control samples consisting of the solutions without brain tissues, as well as the solutions spiked with known quantities of bacterial magnetite, were run to check for contaminants in the solvents as well as to determine their effect, if any, on the well-studied morphology of bacterial magnetites.

RESULTS

Magnetometry. All of the tissues examined had isothermal remanent magnetizations (IRMs) that saturated in applied fields of ≈300 mT, a characteristic property of the magnetite-maghemite series. The ability to gain and lose remanent magnetization in these experiments is a definitive characteristic of ferromagnetic materials. Table 1 shows the mean values for each brain. The average magnetization indicates the equivalent of ≈4 ng of magnetite per gram of tissue. In contrast, average values for the meninges from three brains (Table 1) are nearly 20 times higher, or ≈70 ng/g. For comparison, measurements of IRM from triple-distilled deionized ice cubes yield a background "noise" of ≈0.5 ng/g.

There was remarkable consistency in the IRM measurements for both the brain tissue and the meninges. There was little difference in IRM from one area of cerebral cortex to another or in the cerebral versus the cerebellar cortex. Differences between tissues from the normal brains versus those suspected or confirmed to be Alzheimer disease cases were negligible. Areas of the brain previously reported to have high iron content include the dentate nucleus, the basal ganglia, and areas of the midbrain (24). Samples of these areas had no greater content of magnetic particles than did the cerebellar or cerebral cortex.

Fig. 1 shows magnetic properties for representative tissues, including coercivity determinations (20) (Fig. 1*A*) and a test for intergrain interaction effects using the anhysteretic remanent magnetization (23) (ARM, Fig. 1*B*). Median coercivity values were ≈30 mT, but ranged from 12 (pia from cerebellum) to 50 (basal ganglia) mT, well within the coercivity range for single-domain magnetite. The shift in coercivity distributions, as measured by IRM acquisition and its demagnetization, and the relatively slow tendency to acquire an ARM suggest that the particles *in situ* are in small interacting clumps. Comparison with bacterial control samples suggests between 50 and 100 particles per clump.

Extraction and Electron Microscopy. When viewed under low power through an optical dissecting microscope, black strings of aggregated particles extracted from brain tissues are seen collected at the focus of the magnetic finger device. In shape and morphology, these aggregations are indistinguishable from similar aggregates from the magnetotactic bacterial controls. No magnetic aggregates were observed to collect in the blank tissue-free control samples. Rough volume estimates of the extracted material, made by measuring the length and width of the aggregates and totaling for each chain, agree to within an order of magnitude with estimates from the IRM measurements, implying that the extraction technique was reasonably efficient.

Fig. 2 shows two representative crystal morphologies of the extracted magnetic particles. Grain sizes were bimodal, with 62 of the 70 measured crystals in the 10- to 70-nm range and the remaining 8 with sizes ranging from 90 to 200 nm. Measurements of the TEM shadows from 62 of the smaller particles in one aggregate yielded an average size of 33.4 ± 15.2 nm. Note that this mean value must be biased toward

Table 1. Mean saturated IRM for cerebral cortex and cerebellum tissues from each brain

Tissue	Saturated IRM, μA·m²·kg⁻¹	Magnetite, ng/g	No. of subsamples
Brain			
1	0.14 ± 0.08	3.0 ± 1.4	11
2	0.18 ± 0.10	3.9 ± 2.2	5
3	0.14 ± 0.05	3.0 ± 1.1	5
4	0.27 ± 0.21	5.9 ± 4.6	6
5	0.20 ± 0.09	4.3 ± 2.0	3
6	0.19	4.1	1
7	0.33 ± 0.19	7.2 ± 4.1	2
Meninges			
1	2.5 ± 1.8	54 ± 39	8
2	2.5 ± 1.5	54 ± 33	8
6	5.0	109	1

Data for saturated IRM are expressed as μA·m²·kg⁻¹ (wet weight) (mean ± SD). Occipital samples were from Brodman areas (B.A.) 17, 18, and 19; temporal samples were from B.A. 20, 21, and 22; parietal samples were from B.A. 3, 1, 2, 5, and 7; and frontal samples were from B.A. 4 and 6. Sample sizes ranged from 0.5 g to 22 g. The meninges from samples of brains 1, 2, and 6 were analyzed separately. The ice-cube technique was used for all of the meninges, and on the tissues from brain 2, and for 7 of the 11 samples from brain 1; no difference in results was seen with this technique. Magnetite concentrations were estimated by noting that the saturation remanence should be exactly half of the saturation magnetization for a dispersion of single-domain crystals (21). Brains 1–4 were from normal patients, brains 5 and 6 were confirmed Alzheimer patients, and brain 7 was a suspected Alzheimer patient.

larger sizes because the extraction procedure will discriminate against very small particles that move more slowly through the liquid. Size and shape relationships for all measured particles fall within the single-domain and superparamagnetic fields for magnetite (25). Crystal volume estimates, done by assuming equant particle shapes, imply that the larger particles compose a maximum of ≈85% of the magnetite. Using this distribution data, we estimate that brain tissues contain a minimum of ≈5 million crystals per gram, distributed in 50,000–100,000 discrete clusters. Similarly, the meninges contain a minimum of 100 million crystals per gram, in 1–2 million clusters.

Energy-dispersive x-ray analyses of the crystals gave consistent peaks of Fe, with variable Cu peaks (from the copper TEM grids) and minor Si, Ca, and Cl (probably contaminants from the glassware). Mixed Fe-Ti oxides, which are usually present at least in trace amounts in geologically formed magnetic minerals, were not detected in any of the brain crystals examined. Indexed electron microdiffraction patterns from individual crystals and particle aggregates yield the d-spacings characteristic of magnetite (Fe_3O_4), with smaller particles showing variable oxidation toward the ferrimagnetic solid-solution end member, maghemite (γ-Fe_2O_3). This oxidation probably occurred during the extraction process, as is observed commonly in very fine grained magnetites (22).

Fig. 2A is a TEM image of a clump of small particles from the cerebellum, and Fig. 2B shows a high-resolution TEM image of a well-ordered single-domain maghemite crystal imaged in the [211] zone. It displays several intersecting sets of crystal lattice fringes that appear as fine stripes that run across the image (and are viewed best at a low angle relative to the page). The most prominent set, which runs across the width of the crystal, corresponds to the 4.85-Å spacing of the {111} plane; another set perpendicular to this, running the length of the crystal, has the 2.95-Å spacing of the {022} planes. Note that the [111] direction of the crystal, which is the easy direction of magnetization (22), is parallel to the particle length and that the {111} fringes go completely across the width of the particle without disruption. A superimposed "graininess" is present, along with somewhat ill-defined edges. These are typical features of magnetite crystals formed within magnetosome membranes (26, 27) and are very similar to the single-domain particles in the magnetosome chain structures present in the dermethmoid tissues of salmon (15). Fig. 2C shows the indexed electron-diffraction spot pattern from this crystal.

Fig. 2D shows one of the larger particles, which is ≈200 nm in size. Other particles range up to 600 nm in diameter. Electron microdiffraction indicates that these particles are dominated by a single crystal, with occasional smaller particles adhering to their surface. Their measured size and shapes place them within the single-domain stability field (25). These particles have magnetic orientation energies in the geomagnetic field 20–150 times higher than the background thermal energy kT.

DISCUSSION

Results from these studies indicate that human brain and meninges contain trace amounts of ferromagnetic material. These magnetic particles in the human brain are diffusely and homogeneously distributed over all cerebral lobes, the cerebellum, basal ganglia, and midbrain. The consistency of our magnetic property data from piece to piece of brain tissue and from piece to piece of meninges suggests that the observed moments were not produced by occasional contamination from the environment but were *in situ* ferromagnetic materials distributed in a tissue-characteristic fashion. The magnetic material was in the tissues *prior* to the chemical
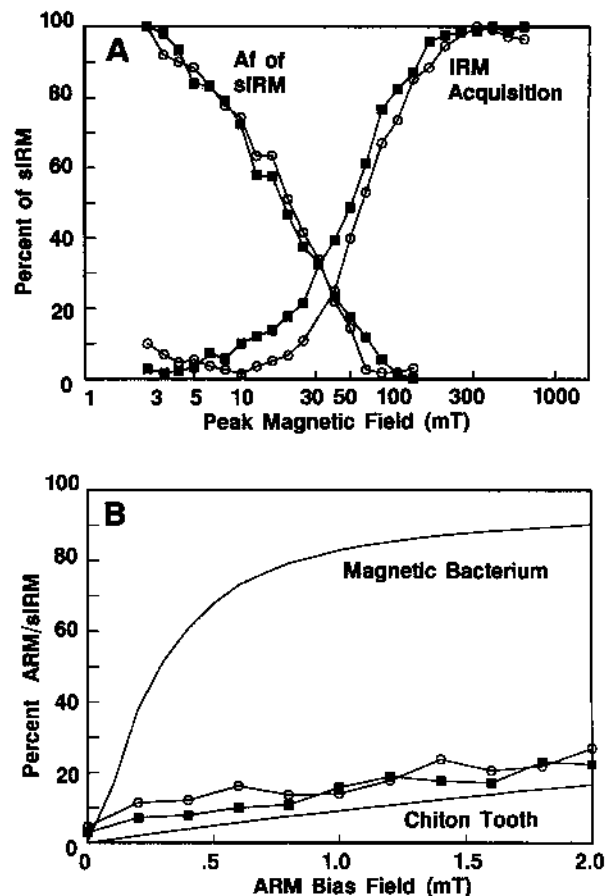

FIG. 1. Rock magnetism of human brain tissues. (A) The curves labeled IRM acquisition show the relative magnetic moments remaining in the samples after a brief exposure to a magnetic pulse of the indicated strength. The tendency of the curves to flatten at high field levels is characteristic of the magnetite–maghemite solid solution series; most other ferromagnetic iron minerals saturate in fields >1 T. The curves labeled Af of sIRM show the progressive alternating-field demagnetization of the saturation IRM. The magnetic field value at which these two curves cross is the best measure of the average coercivity. The ordinate of the intersection point for noninteracting particles occurs at the 50% value; a depression or shift in this position is an indication of particle clumping effects. (B) The acquisition of ARM. The upper control curve shows data from a sample of magnetotactic bacteria in which the magnetite crystals are aligned in linear chains and have few interparticle interactions, whereas the lower control curve is from a sample of magnetite from chiton teeth, which are single-domain crystals but are highly interacting. Solid squares are data from pia from the frontal lobe, whereas the open circles show data from the cerebellum. sIRM, saturated IRM.

digestion steps, which are of the most concern for potential contamination. An external inorganic source is also unlikely because of the lack of particles containing mixed Fe-Ti oxides, which are common in igneous and metamorphic magnetites. Surface textures and crystallographic features for the smaller particles are remarkably similar to biogenic magnetites studied in bacteria (27) and fish (15). The {111} crystal alignment has been interpreted as a biological mechanism for maximizing the magnetic moment per particle, as the {111} direction yields ≈3% higher saturation magnetizations than do other directions (15, 27, 28). This prismatic particle shape is also uncommon in geological magnetite crystals of this size, which are usually octahedra. Hence, these magnetite crystals probably form within human tissues by a similar biologically controlled process. Unfortunately, the tissue digestion and extraction process destroys the
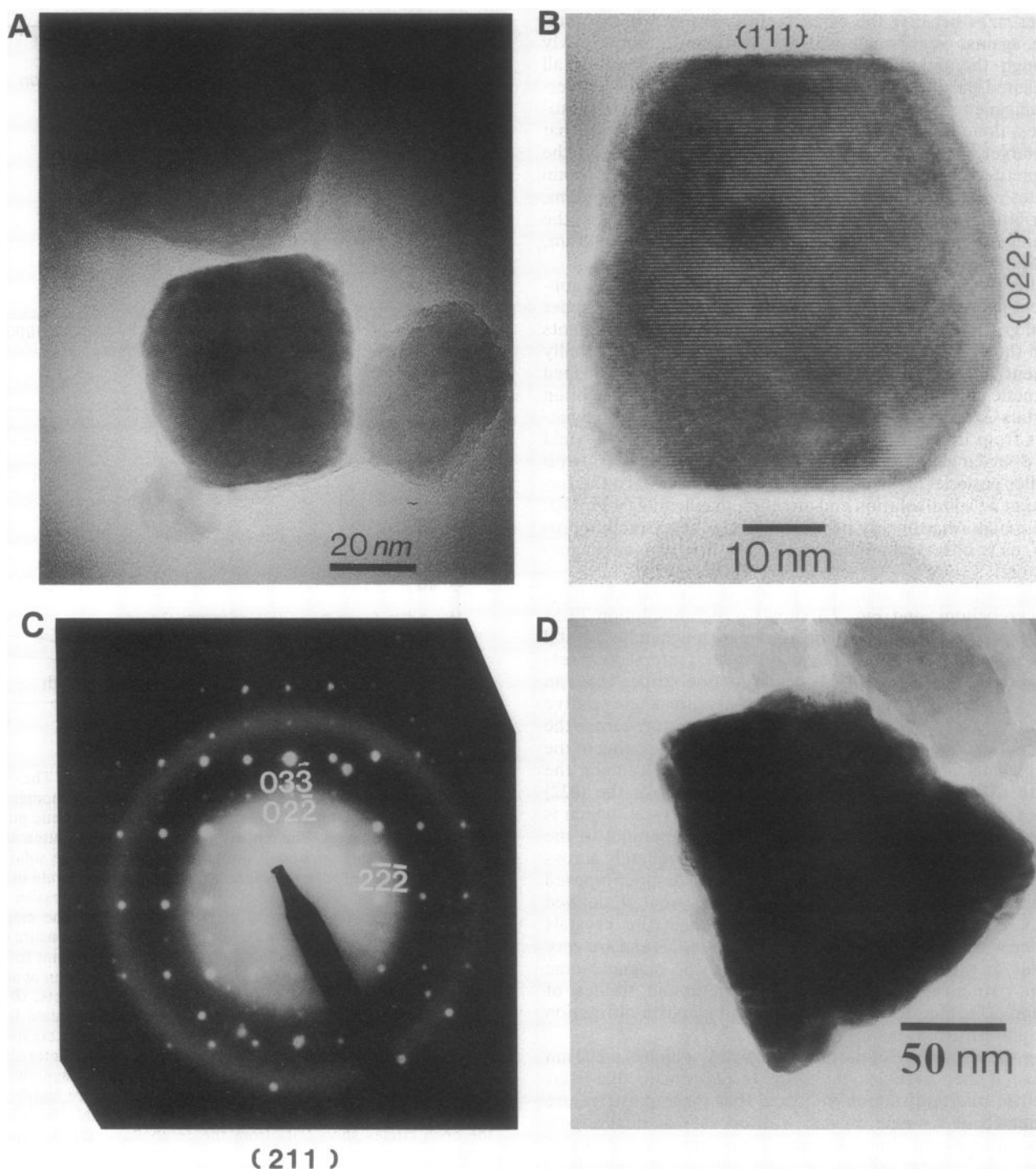
FIG. 2.   TEM images and diffraction patterns of representative magnetite and maghemite crystals from the human cerebellum. (*A*) A clump of small particles. The high-resolution TEM image of the maghemite crystal in *B* shows the pattern of intersecting {111} and {0$\bar{2}$2} fringes, with particle elongation in the [111] lattice direction. (*C*) The indexed selected-area electron diffraction pattern of this crystal, taken in the ⟨211⟩ zone. (A few miscellaneous spots are also present from the adjacent crystals seen in *A*, and the faint row of spots midway between the bright rows are [01$\bar{1}$] and equivalent reflections that indicate the oxidation to maghemite.) The diffraction rings from an aggregate of small crystals confirms the magnetite–maghemite identification. These measured values/γ-Fe$_2$O$_3$ standards/and [indexed] d-spacings for the rings are, respectively, 4.0 Å/4.18 Å [200], 4.8 Å/4.82 Å [111], 3.2 Å/3.41 Å [211], 2.8 Å/2.95 Å [220], 2.6 Å/2.78 Å [221], 2.2 Å/2.23 Å [321], 1.8 Å/1.87 Å [420], 1.7 Å/1.70 Å [422], 1.5 Å/1.61 Å [511], and 1.3 Å/1.32 Å [620]. The tetragonal reflections [211], [221], and [321] are present in maghemite, and not in magnetite, and the pattern from the aggregate is a mixture of the two. One of the large magnetite particles is shown in *D* (diffraction pattern not shown).

cellular organization of the particles. Only the ARM results yield clues to the *in situ* grouping in small clumps.

In recent years, several medical groups have claimed that MRI images weighted by T1 and T2 values correlated with the observed distribution of stainable ferric iron in human brain tissue (2, 29, 30). These anomalous values have been inter-

preted as arising from irregular distributions of paramagnetic iron (deoxyhemoglobin, ferritin, and hemosiderin). Iron distributions measured in this fashion increased with age, as is known from extensive histological work (24). However, this interpretation was challenged subsequently by Chen *et al.* (31), who found generally poor correlation between iron

Biophysics: Kirschvink *et al.*

Biophysics: Kirschvink *et al.*

Proc. Natl. Acad. Sci. USA 89 (1992) 7687

concentration and T2 relaxation, and by Bizzi *et al.* (32), who discovered that the iron-correlated spin echo effects did not have the quadratic variation with increasing magnetic field strength predicted by the paramagnetic hypothesis. All of these results are more compatible with the presence of trace levels of magnetite.

The presence of magnetite in human tissues has potential implications for at least two biomedical issues that have been discussed extensively in the literature; these include human exposure to the strong static fields used in MRI studies (3) and the much weaker 50- and 60-Hz fields produced by the electric power system and appliances in industrialized countries (4–7). (*i*) MRI systems are now being used routinely in clinical applications that subject patients to static background magnetic fields in excess of 1.5 T, 30,000 times stronger than typical geomagnetic fields. Under these conditions the maximum magnetostatic orientational potential energies for the magnetic particle clumps are between 10^3 and 10^7 times higher than the thermal energy kT at body temperature. Hence, the energies are much larger than the chemical energies present in covalent bonds, which typically are on the order of 100 kT. (*ii*) The magnetic torque from external alternating fields will induce mechanical oscillations in the particles, and the potential exists for such motions to have effects like opening transmembrane ion channels. Two separate analytical approaches suggest that fields of 50 or 60 Hz with peak intensities slightly stronger than that of the earth would be required to make these effects stand above kT (7, 33), but the large numbers of crystals might allow averaging to yield effects at lower levels. Although peak alternating magnetic fields generated by most electric transmission lines are well below this level, some electric appliances produce stronger fields (34). Unfortunately, without more knowledge of the cellular location, ultrastructure, or biological function of these particles, it is impossible to predict whether magnetomechanical effects of this sort pose a human health hazard.